Tianjin Daxue Xuebao (Ziran Kexue yu Gongcheng Jishu Ban)/
Journal of Tianjin University Science and Technology
ISSN (Online):0493-2137
E-Publication: Online Open Access
Vol: 55 Issue: 09:2022
DOI: 10.5281/zenodo.19248008

EXPERIMENTAL INVESTIGATION OF 50CrV4 AND SAE 5160 SPRING STEELS ON THE PRECISION AND DURABILITY OF IS-3 SIZE ACTUATORS FOR INDUSTRIAL AUTOMATION

Dr. SURESH JADHAV*
Assistant Professor, Department of Mechanical Engineering VJTI Matunga, Mumbai, India. *Corresponding Author Email: sgjadhav@me.vjti.ac.in

SIDDHESH JAITAPKAR
Department of Mechanical Engineering VJTI Matunga, Mumbai, India.

Dr. SUNIL BHAMARE
Joint Director, Directorate of Technical Education Mumbai, India.

Abstract

The present work is carried out on the design and modelling of IS-3 size actuator under industrial simulated conditions. The two different materials 50CrV4 and SUP9/SAE 5160 are tested for the load capacity of spring at different stroke length. On the other side, the second material selected was 50CrV4 and SUP 9/SAE 5160 with wire diameters of 28 mm and 30 mm and the same procedures were applied and both the results were compared with the standard data. Shear stress and deformation calculated using FEA solver at position 85 of precompression, 50 mm stroke after precompression and 100 mm full stroke after precompression. Finite element analysis was performed to predict the fatigue life behaviour of both springs based on SN curve and strain life parameters. 50CrV4 generally offers better fatigue resistance and less sensitivity to loading conditions compared to SUP9/SAE 5160. This makes 50CrV4 a more suitable choice for helical spring applications where fatigue loading is a critical factor. Obtained results for fatigue life based on mean stress curve methods which gives better predictions under the industrial simulated load conditions.

Keywords: IS-3 Size Actuator**,** FEA, Fatigue Life, 50CrV4 and SUP9/SAE 5160, Stroke Length, Deformation. Positional Accuracy.

1. INTRODUCTION

Industrial valve actuators have an important role in automating and controlling fluid flow in a range of industrial operations. From manual control to today's modern smart actuators, these devices have developed significantly, driven by the demand for increased efficiency, precision, and safety.

Understanding their development and functions aids in optimizing their use in current industrial systems, leading to reliable and efficient process control. The evolution of process control and industrial automation is directly related to the history of pneumatic control valves.

Pneumatic control systems date back to the late 19th and early 20th centuries, marking the beginning of industrial automation. It uses compressed air to regulate mechanical components, such as valves in industrial applications. Illustration of pneumatic actuator for control valve application and cross-sectional view of actuator shown in Fig. **1** and Fig. **2** respectively.

Tianjin Daxue Xuebao (Ziran Kexue yu Gongcheng Jishu Ban)/
Journal of Tianjin University Science and Technology
ISSN (Online):0493-2137
E-Publication: Online Open Access
Vol: 55 Issue: 09:2022
DOI: 10.5281/zenodo.19248008

Fig 1: Pneumatic actuator for control valve

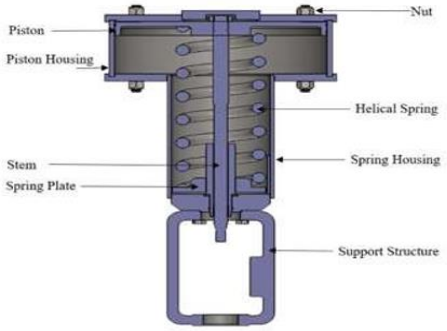

Fig 2: Cross sectional view of actuator

Enhancing industrial valve applications parameters is a broad field of study that includes actuator technology, control systems, material science, flow dynamics, stability, and maintenance strategies. Numerous researchers have endeavoured to address static equations in the static analysis of helical compression springs. Champagne, R.P., et.al. (1996) examined valve actuator parameters to enhance the performance of control valves. Their investigation focused on how factors such as supply pressure, load margin, flow, and actuator size and design influenced outcomes, utilizing mathematical simulations for their analysis. Yang, C.J. et al. (2014) conducted research to create a dynamic model for the numerical analysis of helical compression springs under axial loads, taking into account the interaction between the coils. Their simulations examined both the dynamic and static stress distribution of the springs under various loading scenarios, including situations involving critical contact between the coils. Lelio Della Pietra (1976) studied and examined the coupling between torsional strains in axially loaded cylindrical helical springs [3]. Pietra, L.D.et.al.(1982) were interested to find out dynamic behaviour of axially excited helical springs [4]. In his 1963 study, Wahl analyzed spring wire as a round bar subjected to shear stress and torque, simplifying the problem by focusing on small deformations. He neglected axial and torsional deformations and introduced a correction factor to account for the spring's curvature. This approach aimed to provide a more accurate understanding of stress distribution in springs, influencing later spring design and analysis methodologies [5]. Igor L Krivts et.al examined pneumatic actuating systems for the structure and design of automatic equipment. They focused on pneumatic actuators and analyzed the components, with performance and cost being the key factors influencing the selection of pneumatic technology over other actuation methods. [6]. AM Wahl (1939) proposes a method for calculating the effect of wire or bar curvature on allowed stresses in helical springs using the material's endurance properties. The method based on the basis, which was consistent with known fatigue-test data, that stress-concentration effects caused by wire curvature can be ignored in estimating the static component of applied stress [7]. Cook, R.D., and Young (1985) investigated the twisting moment of a helical spring with a circular cross- section. They assumed that both the transverse shear strain and the direct stretching of the wire were relatively insignificant[8]. Stress analysis is also important consideration during the design of helical

Tianjin Daxue Xuebao (Ziran Kexue yu Gongcheng Jishu Ban)/
Journal of Tianjin University Science and Technology
ISSN (Online):0493-2137
E-Publication: Online Open Access
Vol: 55 Issue: 09:2022
DOI: 10.5281/zenodo.19248008

compression spring. M. Gzal and colleagues (2017)analyzed the stress distribution in helical springs with elliptical cross-sections, considering a very small helix angle and the impact of wire curvature under an applied static axial load. Nagaya, K. (1987) did research on stresses in helical spring. He presented a theoretical result for obtaining stresses in a helical spring due to compression or tension of arbitrary cross section with consideration of end effects [10]. Many research studies and investigations done in the field of stress calculations and its distribution across the coils of helical spring during the loading and unloading conditions. In several studies, a finite element model was created to estimate results that fulfill the governing equations and boundary conditions on the surface of the coil. Zhang, D., et.al developed a finite element model to analyze the mechanical behavior of bolt connections under axial loading. Their work involved creating a detailed simulation that accounted for the various factors affecting the performance of bolt connections, including material properties, geometric configurations, and loading conditions. By using finite element analysis (FEA), they were able to predict the stress distribution, deformation, and potential failure modes of the connections, providing valuable insights for engineering applications and design optimization. This model can be useful for improving the reliability and safety of structures that utilize bolt connections in various fields, such as civil, mechanical, and aerospace engineering. Many research theories proposed on the fasteners to find out the stress behaviour across the threads [15-17].

Baran, R. and colleagues (2023) published a paper focusing on the experimental analysis of the distribution in cylindrical helical compression springs with specified geometric parameters. They investigated the influence of number of active coils and end coil design on stiffness distribution [18]. Zebdi, O.et.al (2009) implemented multi objective evolutionary algorithm to reduce the mass and increase the spring stiffness [19]. Gobbi, M. and Mastinu, G. (2001) presented and developed mathematical model for helical spring design. This method defines geometrical and mechanical parameters based on technical specifications such as stiffness of the spring, maximum defection to achieve the better performance of the spring to maintain the spring stability [20].

The fatigue life prediction of helical compression springs is a well-explored research topic. Del Llano Vizcaya and Rubio-González (2006) utilized multiaxial fatigue criteria to analyze these springs. Through experimental testing, they identified the initiation point of fatigue cracks and used numerical methods to predict the areas experiencing the highest damage [21]. Akiniwa Y.et.al (2008), evaluated the fatigue strength and fracture strength of smooth valve spring steel specimens that fatigued up to the giga cycle regime under axial and torsional stresses [22]. In their 2006 study, Berger and Kaiser examined the outcomes of very high cycle fatigue tests conducted on shot-peened helical compression springs. These springs are subjected to external compressive loads that generate torsional stresses. The findings offer significant insights into the fatigue performance of helical compression springs [23]. M.T. Todinov (1999) proposed an equation to calculate the maximum tensile stress exerted on helical compression springs under loading. He developed a method for identifying the origins of fatigue cracks in these springs and examined how shot peening—a surface treatment technique—affects the locations of these fatigue crack origins, ultimately contributing to improved fatigue resistance in the

Tianjin Daxue Xuebao (Ziran Kexue yu Gongcheng Jishu Ban)/
Journal of Tianjin University Science and Technology
ISSN (Online):0493-2137
E-Publication: Online Open Access
Vol: 55 Issue: 09:2022
DOI: 10.5281/zenodo.19248008

springs. Melander, A. and Larsson, M. (1993) conducted tests on hardened spring steel subjected to fully reversed loading at five distinct stress amplitudes. They developed a model to predict the failure probability of fatigue test specimens, which illustrates the crack growth around pores. Gomes and Souto (2016) examined the monotonic and fatigue characteristics of 51CrV4 spring steel, focusing on its use in leaf springs. They utilized fatigue models grounded in strain-life and energy methods to evaluate the material's performance across various loading conditions. Their findings provide essential insights into the steel's reliability and durability, aiding in the design and application of leaf springs to ensure they can withstand cyclic loads without failure. Lot of studies and researches done till now to find the fatigue behaviour of materials under different conditions. Numerous researchers have concentrated on prototype testing and developed fatigue failure criteria, including design formulas and equations, to address the pressing need for fatigue-resistant designs [27–28]. Jhansale, H.R., and Topper, T.H. (1971) investigated the inelastic stress response under cyclic strain conditions and proposed a novel approach for determining the geometry of the hysteresis loop [29]. Li, D.M., et.al. (1998) investigated low cycle fatigue behaviour of high strength spring steel to get the idea about fatigue damage mechanism based on strain energy approach [30]. Many research studies done on low cycle fatigue of high strength material followed by evaluation of fatigue parameters suitable for fatigue life estimation under different loading conditions. Many experimental research studies on strain controlled low cycle fatigue conducted to evaluate strain life parameters [31-34]. Some models with equations developed to determine the relation between stress-strain curve and strain life curve to describe the fatigue behaviour of material at specific loading conditions [35-36].

In current research study, the main focus is on the design, development, optimization and validation of an IS-3-sized actuator for precision control in industrial applications. The work involves the design of a helical compression spring for a pressure load of 9 kg/cm^2. Initially, the material selected was 50CrV4 with a wire diameter of 28 mm, and load tests were conducted to find the load carrying capacity of the spring and the stiffness of the coil at increasing load until the solid length. The FEA-based analysis under load amplitude was done to find out the fatigue life of the spring on the basis of the SN curve method and strain life parameters with the help of previous research data. On the other side, the second material selected was SUP 9/SAE 5160 with wire diameters of 28 mm and 30 mm and the same procedures were applied and both the results were compared with the standard data. The maximum stresses developed due to the spring used to design the spring housing, piston housing, stud design and minimum weld size. This research attempts to innovate the design and optimize the cost-effectiveness of pneumatically controlled actuators, aiming to enhance their performance, reliability, and affordability.

2. FEA ANALYSIS

FEA based analysis mainly consists of analysis of spring, spring and piston housing, piston, weld and stud-nut at higher stresses (9 kg/cm^2). By applying different materials for different parts analysis done by using ANSYS software. Table **2** shows the material selection for various parts of actuator body.

Tianjin Daxue Xuebao (Ziran Kexue yu Gongcheng Jishu Ban)/
Journal of Tianjin University Science and Technology
ISSN (Online):0493-2137
E-Publication: Online Open Access
Vol: 55 Issue: 09:2022
DOI: 10.5281/zenodo.19248008

Material for actuator parts

Table 2: Selection of material for actuator parts

Sr. No	Part name	Material /Specification	Size	Allowable stress
1	Piston	IS 2062 Gr. B	Ø435.74 x 38.5L	137 MPa
2	Piston Housing Finish	Carbon steel	Ø457.20 x 156.25L	137 MPa
3	Spring Housing Finish	Carbon steel	Ø219.02 x 340L	137 MPa
4	Stud	ISO 898 Gr.10.9/8.8	M20 x 2.5P x 240L	137 MPa
5	Nut	ISO 898 Gr.10/8	M20 x 2.5P	137 MPa

Fig. 3 shows boundary conditions applied for calculating maximum stresses. Total pressure of 0.8825 MPa (9 Kg⁄cm^2) applied at inside area of piston housing and 0.3 MPa (3 Bar) at the area where spring's lower end touches the spring housing (0.3 MPa is the maximum pressure when the spring experiences maximum stresses).

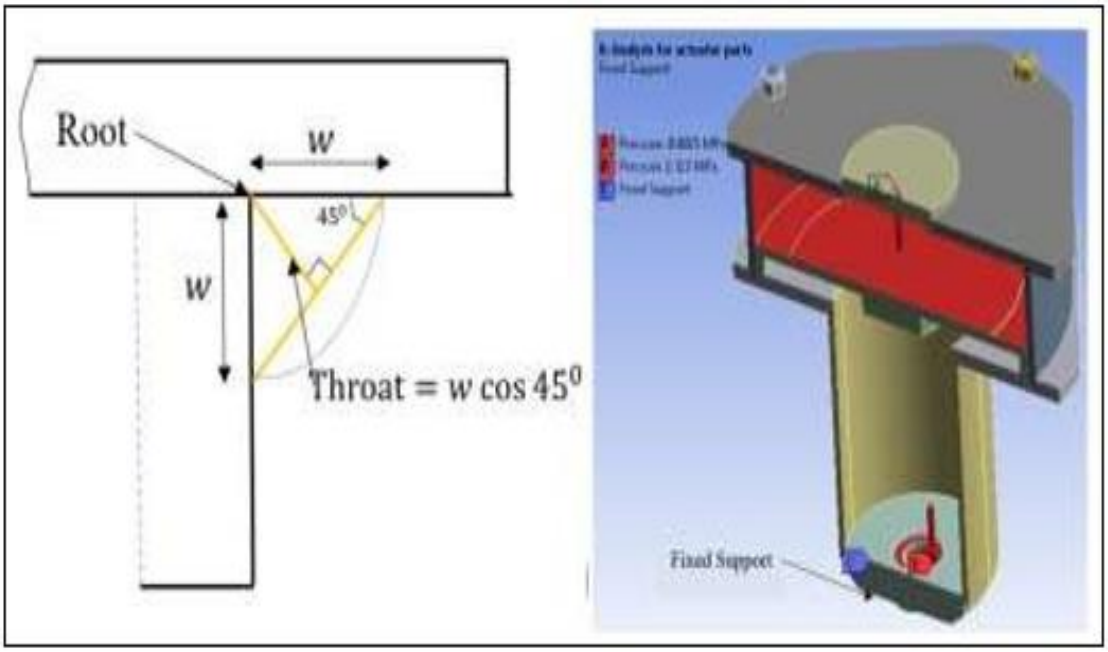

Fig 3: Geometry of fillet weld and boundary condition (pressure input)

Carbon steel having density 7800 Kg⁄m^3, Youngs' modulus 2e+11 Pa and 0.3 Poisson's ratio selected for the stress analysis of piston housing and spring housing with allowable stress of 137 MPa. Maximum stress calculated with 5 mm element size and fine meshing quality.

Fig. 4 shows structural analysis for piston housing.The piston shows a maximum stress of 117.21 MPa (below the 137 MPa allowable) and minimal deformation (0.40 mm) because of a strong, well-designed structure, using high-strength materials, optimized geometry, and built-in safety factors. It performs safely under pressure without risk of failure

Tianjin Daxue Xuebao (Ziran Kexue yu Gongcheng Jishu Ban)/
Journal of Tianjin University Science and Technology
ISSN (Online):0493-2137
E-Publication: Online Open Access
Vol: 55 Issue: 09:2022
DOI: 10.5281/zenodo.19248008

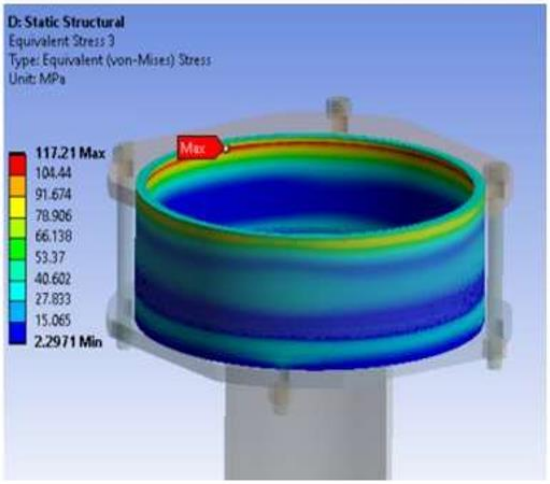

Fig 4: a) Stress in piston housing

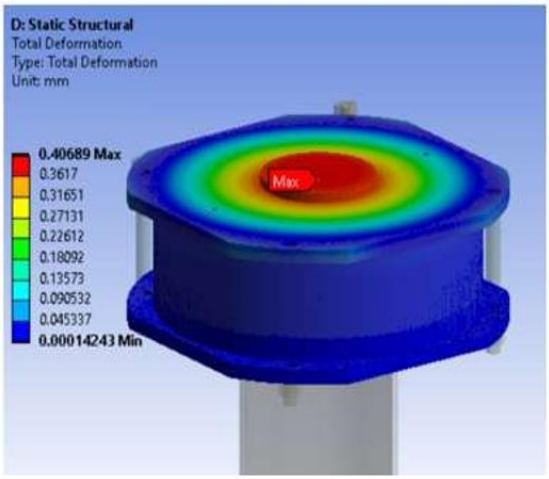

Fig 4: b) Maximum deformation in piston housing

Fig.5 shows structural analysis of spring housing. Maximum stress in spring housing observed is 12.847 MPa which is far lower than allowable stress, indicating design can withstand higher pressure load. the lower observed stress compared to the allowable stress reflects a prudent approach that prioritizes safety and reliability, ensuring the component can handle higher pressure loads without failure.

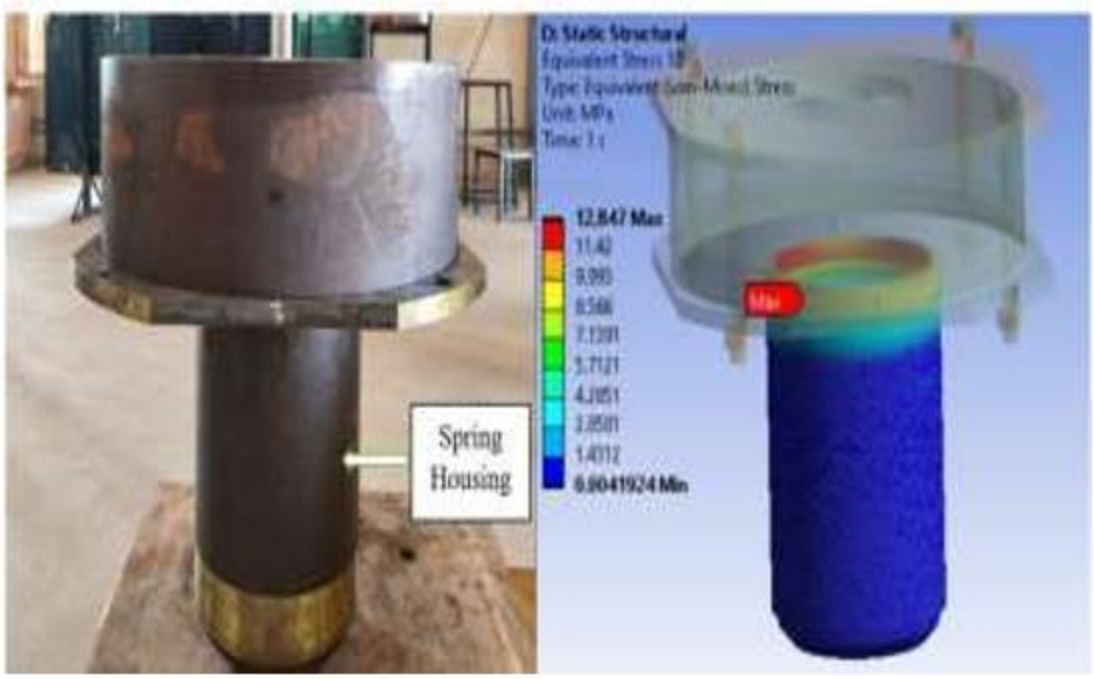

Fig 5: Structural analysis of spring housing

Tianjin Daxue Xuebao (Ziran Kexue yu Gongcheng Jishu Ban)/
Journal of Tianjin University Science and Technology
ISSN (Online):0493-2137
E-Publication: Online Open Access
Vol: 55 Issue: 09:2022
DOI: 10.5281/zenodo.19248008

Piston with material IS2062 Grade B having density 7850 Kg/m^3 Youngs' modulus 2e+11 Pa and Poisson's ratio 0.32 selected for structural analysis with same allowable stress of 137 MPa. Fine mesh with element size of 2 mm selected for maximum stress calculation.

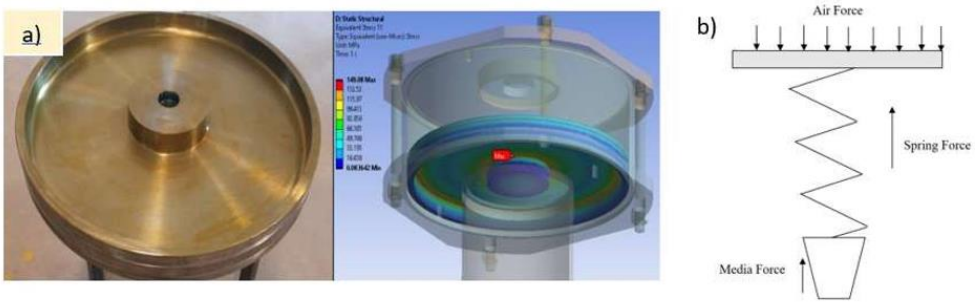

Fig 6: Structural analysis of piston at higher pressure

From above Fig. 6 (a) analytical value for maximum stress is 149.08 MPa which is more than allowable stress value (137 MPa). Observed value is higher at area where spring touches piston at spindle. Fig. 6 (b) illustrates forces acting on piston. Spring force acting on one side of piston and air pressure on other side. Media force which transmitted through valve acts centrally on piston, is applied at piston's center where the spindle connects. The spring force concentrated at the point only where the spring end touches the piston, where the air pressure on other side is thought to be uniformly distributed, due to which valve plug remains in its particular open position. Media force is difference between air force and spring force. The stress by analytical method which is higher above allowable limit is neglected and hence design considered as safe for remaining stress values. The stud specifically chosen from ISO 898, Grade 10.9 and nut from ISO 898, Grade 8.8 having density 7800 Kg/m^3, Youngs' modulus 2.1e+11 Pa and Poisson's ratio 0.3 and selected mesh with element size 2 mm and fine mesh quality. Similar method used to calculate stress in designed weld at higher pressure shown in Fig. 7. In upper portion of fillet weld, maximum von-mises stress found at top is 12.481N/mm^2 and minimum at the bottom 8.12 N/mm^2.Lower portion of fillet weld maximum von-mises stress found at top is 0.9234 N/mm^2 and 0.185 N/mm^2 at higher pressure. Upper portion of stud maximum von- mises stress found at top is 200.01 N/mm^2 and Lower portion of stud minimum von-mises stress found is 0.00027 N/mm^2 at higher pressure. The upper fillet weld shows higher Von Mises stress likely due to uneven load distribution**,** weld geometry differences**,** or stress concentration from the way the load or pressure is applied. The lower weld is less stressed, possibly because it's shielded from the main force or has better load sharing.

2.1 Helical compression spring analysis

The material used in current study for analysis is SUP 9/SAE 5160 and 51CrV4. Chemical composition and material properties are shown in Table 3 and Table 4 respectively. Applied pressure on piston is 0.1320 MPa, 0.2097 MPa and 0.2874 MPa respectively (observed spring range 0.13-0.28 MPa).

Tianjin Daxue Xuebao (Ziran Kexue yu Gongcheng Jishu Ban)/
Journal of Tianjin University Science and Technology
ISSN (Online):0493-2137
E-Publication: Online Open Access
Vol: 55 Issue: 09:2022
DOI: 10.5281/zenodo.19248008

Shear stress and deformation calculated using FEA solver at position 85 of precompression, 50 mm stroke after precompression and 100 mm full stroke after precompression as shown in Fig.7.

Shear stress and deformation calculated using FEA solver at position 85 of precompression, 50 mm stroke after precompression and 100 mm full stroke after precompression Maximum shear stress 447.35 MPa ,730.68 MPa and 1092.1 MPa and deformation 87.92mm,139.19mm, and 189.94 mm are found after precompression at different position such as 50mm 85 mm,100mm.

After full stroke precompression, the material enters plastic deformation, causing shear stress and deformation to rise rapidly due to loss of stiffness and stress concentration in the weld.

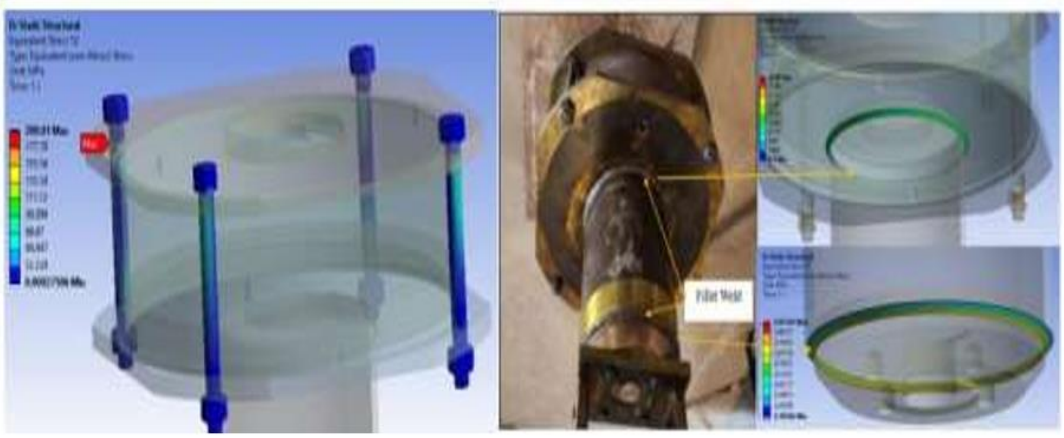

Fig 7: Shear stress and deformation for spring with 50CrV4 material

It has been observed from Table 5, SUP 9 has lower shear stress and deformation compared to 50CrV4 likely because it has higher toughness, better ductility, or more favorable microstructure for absorbing loads, even if both are spring steels. It may also have lower stiffness, allowing it to flex more without concentrating stress.

Table 5: FEA based results for shear stress and deformation

Compression Length	Shear Stress in N/mm^2		Deformation in mm	
	Spring 1 (50CrV4)	Spring 2 (SUP 9)	Spring 1 (50CrV4)	Spring 2 (SUP 9)
85 mm	447.35	395.63	87.95	86.32
135 mm	730.68	628.27	139.19	136.53
185 mm	1092.1	929.7	189.94	186.46

From Fig.9 (a) and (b) it has been seen that pressure and compression length for spring with material 50CrV4 and SUP 9 increases its shear stress also increases deformation. Increasing pressure and compression length increases the load on the spring, which leads to higher shear stress and deformation due to greater internal force and strain. Fig.11 clears that, for shorter compression lengths the mathematical analysis closely approximates the FEA results.

Tianjin Daxue Xuebao (Ziran Kexue yu Gongcheng Jishu Ban)/
Journal of Tianjin University Science and Technology
ISSN (Online):0493-2137
E-Publication: Online Open Access
Vol: 55 Issue: 09:2022
DOI: 10.5281/zenodo.19248008

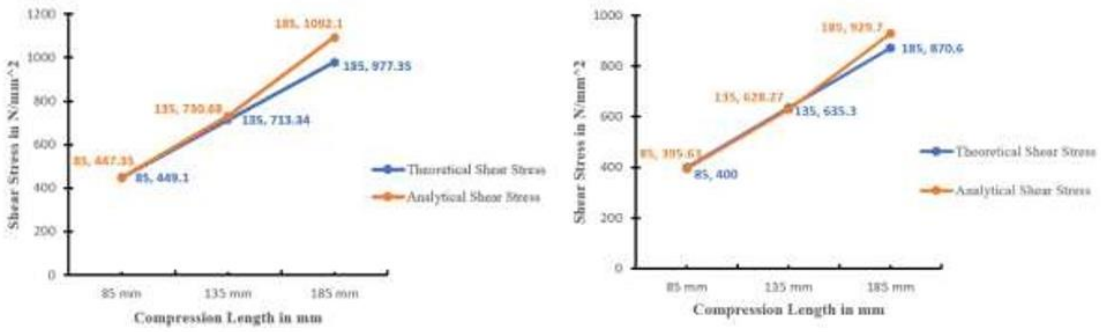

a) Comparison of shear stress vs compression length for spring with material 50CrV4 and SUP 9 respectively

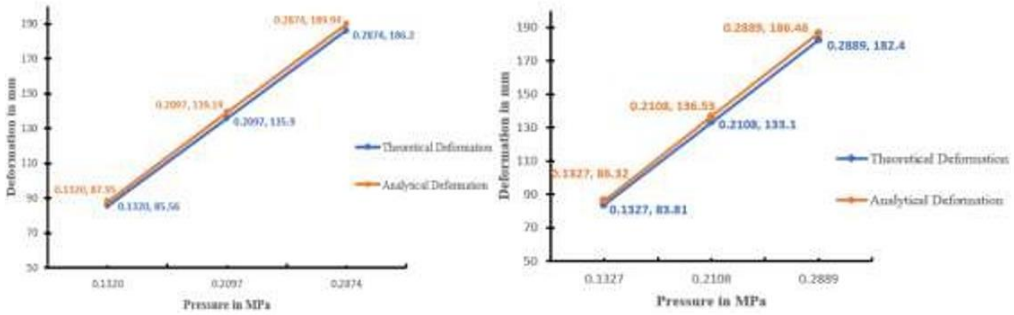

b) Comparison of pressure vs actual deformation for spring with material 50CrV4 and SUP 9 respectively

Fig 8: Comparison of FEA and analytical analysis for shear stress and deformation

2.2 Fatigue life prediction by FEA based method

Finite element analysis was performed to predict the fatigue life behaviour of both springs based on SN curve and strain life parameters. Strain based approach involves determining a relationship between cyclic strain given to material and number of cycles it can withstand before breaking due to fatigue based on equation (8) and equation (9). Alternating stress vs number of cycle data and strain life parameters for SUP 9 material and 50CrV4 material listed in Table 6 and Table 7 respectively.

Table 6: SN data and strain life parameters for SUP 9 material

SN Data		Strain life parameters	
Cycles	**Alternating Stress in MPa**	**Parameters**	**Value**
1	1584	Strength Coefficient	2063 MPa
1000	1123.096	Strength Exponent	-0.08
1E+08	447.1125	Ductility Coefficient	9.56
1E+11	257.2864	Ductility Exponent	-1.05
		Cyclic Strain Hardening Exponent	0.13
		Cyclic Strength Coefficient	2432 MPa

Tianjin Daxue Xuebao (Ziran Kexue yu Gongcheng Jishu Ban)/
Journal of Tianjin University Science and Technology
ISSN (Online):0493-2137
E-Publication: Online Open Access
Vol: 55 Issue: 09:2022
DOI: 10.5281/zenodo.19248008

Table 7: SN data and strain life parameters for 50CrV4 material

SN Data				Strain life parameters	
Cycles	**Alternating Stress in MPa**	**Cycles**	**Alternating Stress in MPa**	**Parameters**	**Value**
10	2937.97	5000	342.899	Strength Coefficient	1100 MPa
20	2237.97	10000	307.391	Strength Exponent	-0.093
50	1608.99	20000	251.594	Ductility Coefficient	0.478
100	1224.49	50000	202.899	Ductility Exponent	-0.684
200	944.493	100000	181.594	Cyclic Strength Coefficient	1476 MPa
500	700	200000	167.391	Cyclic Strain Hardening Exponent	0.0651
1000	545.797	500000	154.203		
2000	433.188	1000000	140		

Results obtained from FEA method depicted in **Fig. 9** and **Fig.10** for selected materials. Fatigue life decreases from precompression → half stroke → full stroke because as stroke length increases, the stress range and strain amplitude also increase, leading to more fatigue damage per cycle. Higher stroke = more material loading and unloading = faster fatigue. So, longer strokes reduce fatigue life in both 50CrV4 and SUP 9 materials.

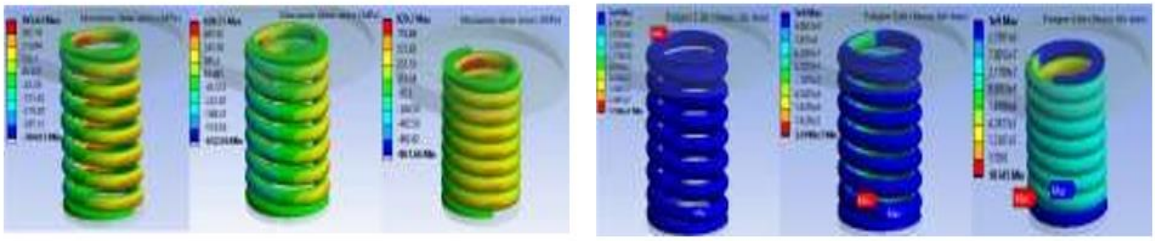

Fig 9: Fatigue life on SN data at precompression (85 mm), half stroke length (50 mm) and full stroke length (100 mm) after precompression for spring with SUP 9 material

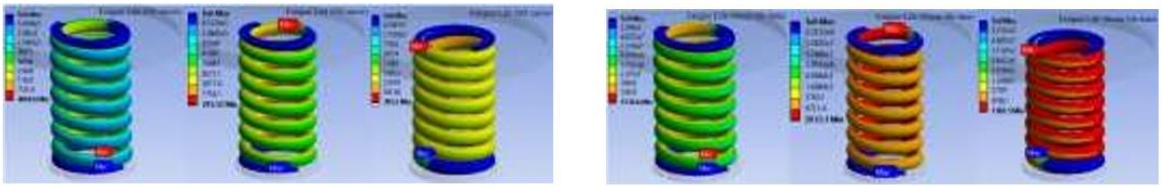

Fig 10: Fatigue life at precompression (85 mm), half stroke length (50 mm) and full stroke length (100 mm) after precompression for spring with 50CrV4 material

3. EXPERIMENTAL ANALYSIS

Experimental analysis mainly focuses on spring's performance under various load conditions and evaluate the spring's compression at corresponding cycles that fall within its operating pressure range. Spring's behaviour under different loading conditions can better understood by subjecting it to different load testing and calculating its stiffness. In

Tianjin Daxue Xuebao (Ziran Kexue yu Gongcheng Jishu Ban)/
Journal of Tianjin University Science and Technology
ISSN (Online):0493-2137
E-Publication: Online Open Access
Vol: 55 Issue: 09:2022
DOI: 10.5281/zenodo.19248008

current experimental study, stiffness of selected coils precisely calculated by applying loads and calculation of resulting deformation which further gives in-depth comprehension of the spring's mechanical properties and failure characteristics. This section describes load testing setup, procedure followed during load testing and methodology used to calculate spring stiffness.

3.1 Experimental setup and procedure

The load test was carried out using setup which designed to calculate the stiffness of spring as shown in Fig. 11. Test involves first and second coil of spring with 85 mm precompression for spring with diameter 28 mm and 30 mm. Load gradually applied to simulate the procedure. Four separate trials were taken, each trial includes 10 observations of loading. Each trial with 10 observations reflects load bearing behaviour under compression. After completion of test, maximum difference between observations in each trial calculated. The ratio of maximum difference to total stroke length taken, which yielding stiffness of spring in kg/mm. This observed stiffness is directly related to potential for spring failure in practical applications.

Fig 11: Illustrates experimental setup for load cycle test on spring with 50CrV4 material

3.3.1 Load cycle test

Fig 12: Load cycle experimental setup

Tianjin Daxue Xuebao (Ziran Kexue yu Gongcheng Jishu Ban)/
Journal of Tianjin University Science and Technology
ISSN (Online):0493-2137
E-Publication: Online Open Access
Vol: 55 Issue: 09:2022
DOI: 10.5281/zenodo.19248008

3.2 Load and stroke length test on spring for spring material SUP 9 and 50CrV4

Fig. 12 (a-d) represents load vs stroke length data of spring specimens obtained through load testing.

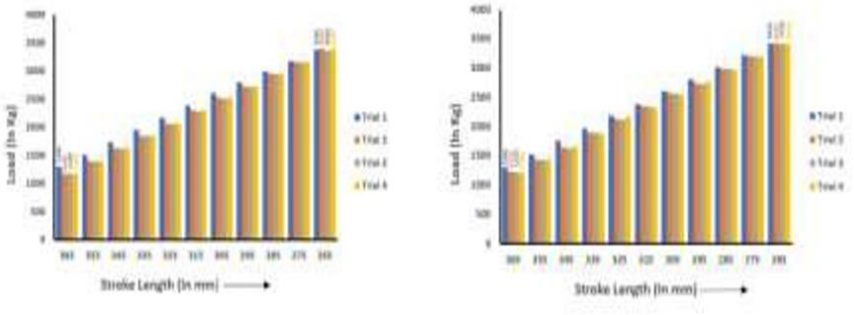

(a) Load test on first and second coil of spring, 28 mm diameter of SUP 9 material

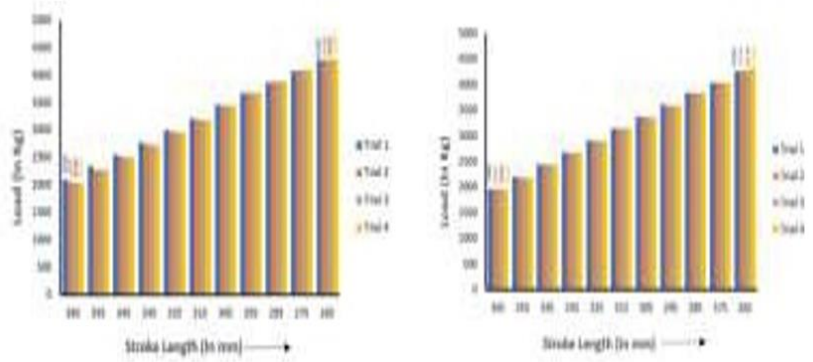

(c) Load test on first and second coil of spring, 30 mm diameter and SUP 9 material

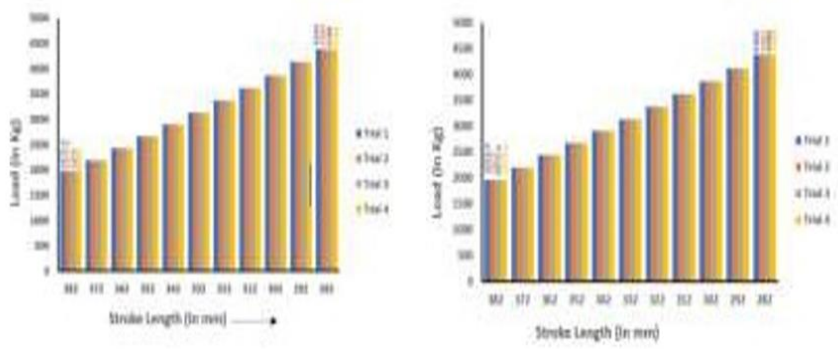

(e) Load test on first and second coil of spring 30 mm diameter of 50CrV4 material

Fig 13: Load test representation

Tianjin Daxue Xuebao (Ziran Kexue yu Gongcheng Jishu Ban)/
Journal of Tianjin University Science and Technology
ISSN (Online):0493-2137
E-Publication: Online Open Access
Vol: 55 Issue: 09:2022
DOI: 10.5281/zenodo.19248008

Stiffness values derived from load experiments presented in **Table 8**. The relation between applied pressure load, compression, stroke length and stiffness illustrated in **Fig. 14** and 15

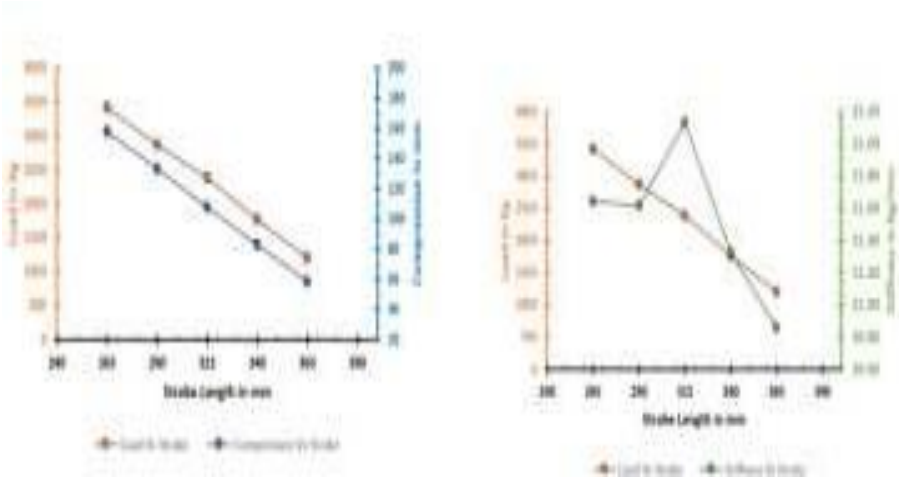

(a) Load – stroke – compression and load – stroke – stiffness relation for SUP 9 spring, 28 mm diameter

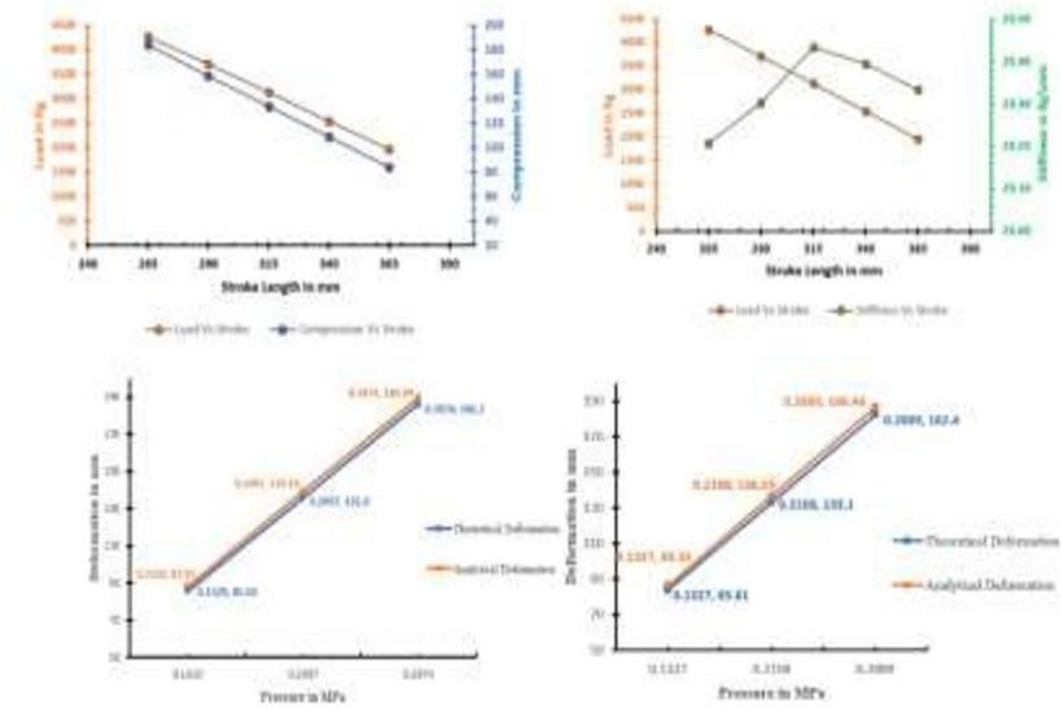

(b) Load – stroke – compression and load – stroke – stiffness relation for SUP 9 spring, 30 mm diameter

Fig 14: Load – stroke – compression – stiffness relation for SUP 9 spring

Tianjin Daxue Xuebao (Ziran Kexue yu Gongcheng Jishu Ban)/
Journal of Tianjin University Science and Technology
ISSN (Online):0493-2137
E-Publication: Online Open Access
Vol: 55 Issue: 09:2022
DOI: 10.5281/zenodo.19248008

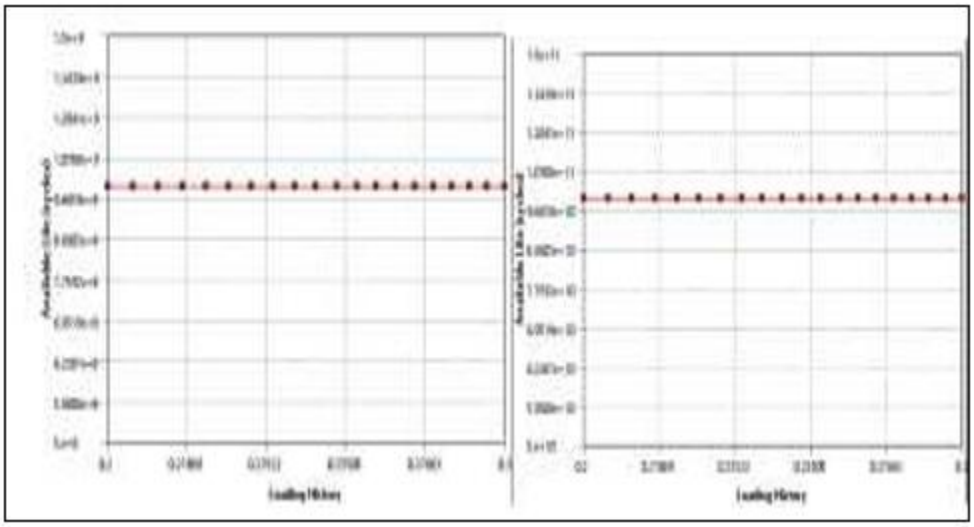

a) Fatigue life at 50 mm and 100 mm stroke length after precompression

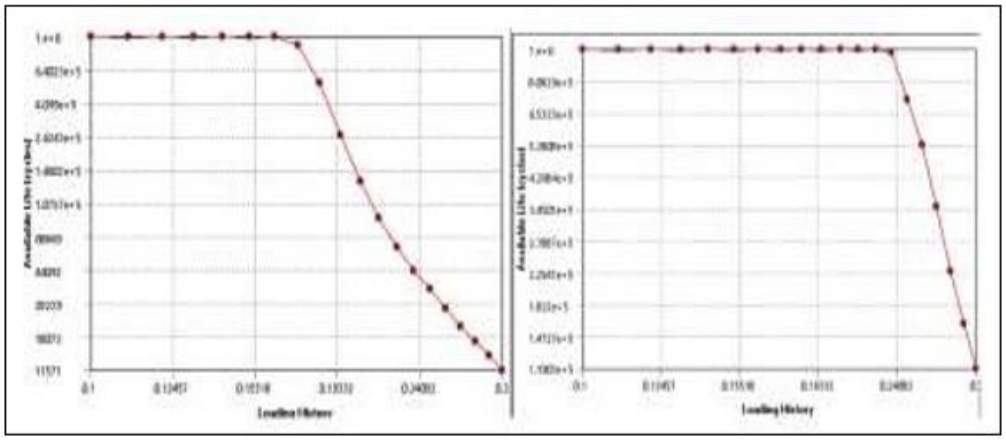

Fig 14: Experimental analysis of fatigue sensitivity life at 50 mm and 100 mm stroke length after precompression for a spring SUP 9 material

Above Fig. 14 demonstrates the relation between load, stroke length, compression and stiffness. The specified designed value of stiffness was 23.5 ± 5% kg/mm. The values obtained from test experiments do not meet the required values. It was also observed that there were small variations in forward and backward stroke indicated discrepancy in performance of the spring. Notably, the variations in SUP 9 spring with diameter 28 mm and 30 mm were observed. These variations are implicated to pre failure of spring, falling short of designed life.At higher pressure load spring exhibited lateral displacement of coils which is commonly known as spring parallelism effect. It was also observed that at higher pressure load spring was unable to take designed load due to deviations in spring squareness. These factors were identified as contributing factors to spring failure. Failure of spring at higher pressure and parallelism effect is depicted in Fig. 15.

Tianjin Daxue Xuebao (Ziran Kexue yu Gongcheng Jishu Ban)/
Journal of Tianjin University Science and Technology
ISSN (Online):0493-2137
E-Publication: Online Open Access
Vol: 55 Issue: 09:2022
DOI: 10.5281/zenodo.19248008

Fig 15: Failure of spring due to parallelism effect at higher pressure load

Figure shows, at solid length due to deviation in parallelism adjacent coils touch each other and releases energy. When theoretical load applied at solid length, coil with more deviation subjected to lateral force, exerted by its adjacent coils A and B. With further increase in load leads to failure of spring as shown in Fig. 15. Experimental study of load cycle test on spring with 50CrV4 discussed in further parts.

3.3 Experimental study on spring material 50CrV4 and SUP9

The load tests were done to calculate the required cycles of spring. Before cyclic test spring tested for shot peening. After shot peening, powder coating was done at 205^{o}C furnace temperature for ideal coating thickness of 90 − 130μm. Powder coating followed by cross hatch test was conducted to ensure the adhesion quality and optimal performance during experiments. Scragging operation on same spring was conducted for removing initial set. Fig. 16 shows the tested samples for cross hatch test.

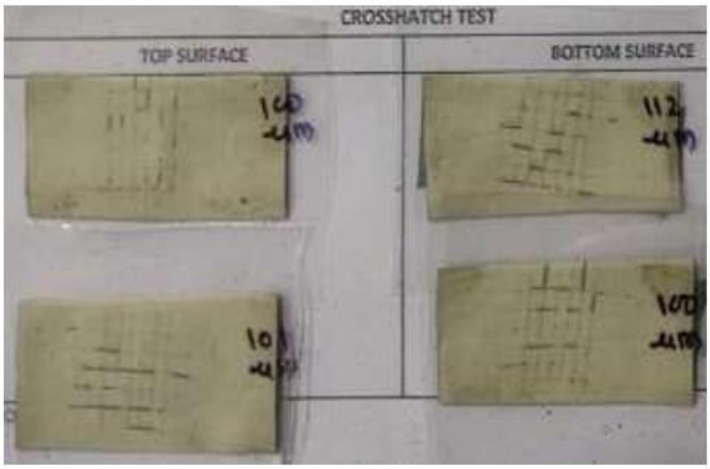

Fig 16: Cross hatch test samples

The load test conducted in four different trials on spring with diameter 30 mm to calculate the stiffness. The load vs stroke length data shown in Fig.16 (e) and (f). Stiffness values derived from experiments listed in Table 9. Results obtained from load test is presented

Tianjin Daxue Xuebao (Ziran Kexue yu Gongcheng Jishu Ban)/
Journal of Tianjin University Science and Technology
ISSN (Online):0493-2137
E-Publication: Online Open Access
Vol: 55 Issue: 09:2022
DOI: 10.5281/zenodo.19248008

in Fig. 17 illustrating the relationship between pressure load, stroke length, compression and stiffness. The load cyclic tests were done on Air to Close (ATC) and Air to Open (ATO) actuators at pressure ranges from 1.14 kg/cm^2 (0.12 MPa) to 3 kg/cm^2 (0.29 MPa).

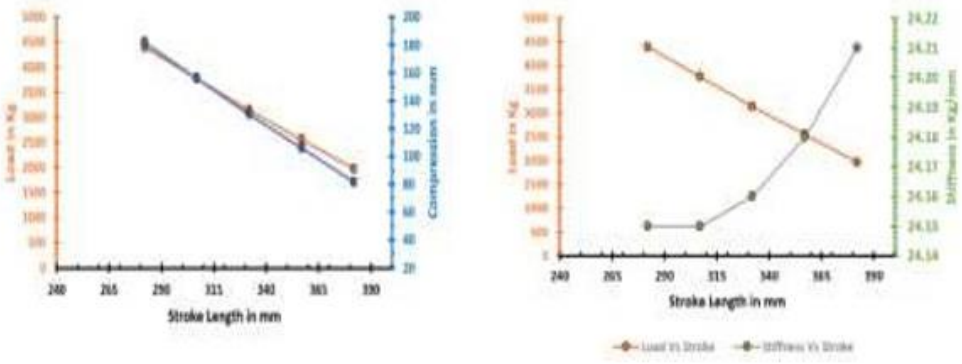

Fig 17: Load – stroke – compression and load – stroke – stiffness relation for 50CrV4 spring, 30 mm diameter

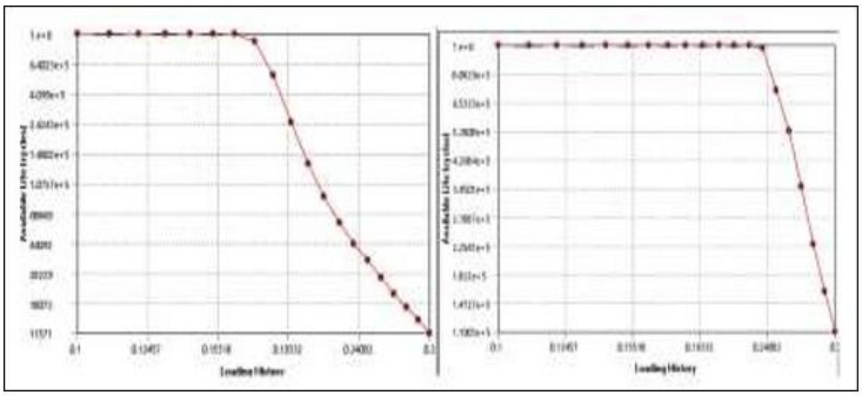

Fig 15: Analysis of fatigue sensitivity for spring 50CrV4 material

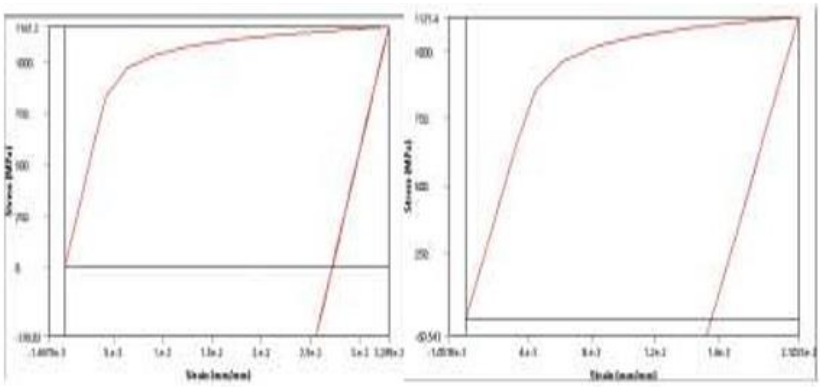

Fig 17: Hysteresis loop at 50 mm and 100mm stroke length after precompression for spring 50CrV4 material

Tianjin Daxue Xuebao (Ziran Kexue yu Gongcheng Jishu Ban)/
Journal of Tianjin University Science and Technology
ISSN (Online):0493-2137
E-Publication: Online Open Access
Vol: 55 Issue: 09:2022
DOI: 10.5281/zenodo.19248008

Figure shows the relation between data of load, stroke length, compression and stiffness obtained through load test. From the figure it is clear that stiffness values calculated from test data and designed values are within the described range (23.5 ± 5% kg/mm). It was also observed that very less variations in forward and backward strokes. One complete forward and backward stoke of actuator's stem gives one complete cycle. The test conducted until 10000 cycles with observations taken after each 500 cycles. During test values of spring squareness (e_1) and spring parallelism (e_2) were measured. Table 10 presents experimental load cycle data for ATC and ATO actuator. From the load cycle experiments it was observed that, no indication of failure or significant variation found in actuators operation until 10000 complete cycles. After completion of test spring length in ATC type actuator was 0.5 mm shorter than initial length and for ATO type actuator it was 4 mm shorter than original length as shown in Fig. 18. These small variations were under limit and acceptable until complete test run.

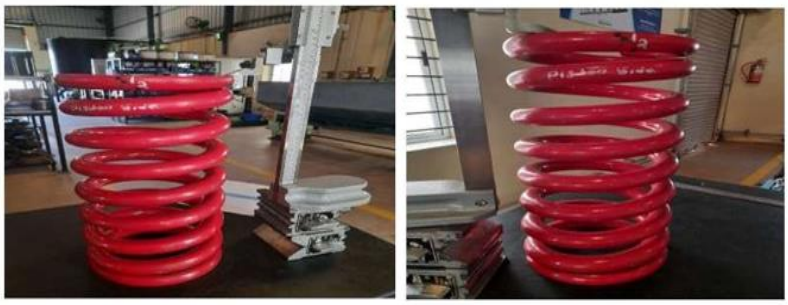

Fig 18: Variations in spring length after load cycle test

4.3.2 Spring linearity and hysteresis test

Spring linearity defines property of spring where displacement from initial position exactly proportional to force used to compress or extend of spring. Spring must pass through equal intervals/gaps of stroke length during loading and unloading at respective pressure. Hysteresis is a phenomenon where position of spring must be same during the loading and unloading at same pressure. Test conducted at pressure range of 1.1 kg/cm^2 (0.11 MPa) to 2.9 kg/cm^2 (0.284 MPa) in four equal intervals. Three trials were performed and observations noted using electropneumatic positioner as depicted in Fig. 19.

Fig 19: Linearity, hysteresis and trueness test setup

Tianjin Daxue Xuebao (Ziran Kexue yu Gongcheng Jishu Ban)/
Journal of Tianjin University Science and Technology
ISSN (Online):0493-2137
E-Publication: Online Open Access
Vol: 55 Issue: 09:2022
DOI: 10.5281/zenodo.19248008

It was observed that maximum percentage of linearity was 5.37%. Actual spring range observed was 1.14 to 3 kg/cm^2. 100 mm lift was observed at 2.92 kg/cm^2. Maximum percentage of hysteresis 7.29% observed at 1.1 kg/cm^2 where stem actually starts to move. These observations were under limit as per designed data. Spring stem movement trueness was evaluated at same pressure range at four different positions. The observations noted were satisfactory, which indicates stem maintained its alignment under varying load conditions.

Table 11: Data obtained from experiment Spring linearity and hysteresis

Pressure	Required(L)	Forword Stroke(A)	Backword Stroke(B)	Lift LA	L - A	A - B	% of Linearity	% of Hysteresis
1.1	0	135.42	145.3	0	0	9.88	0	7.295820411
1.5	25	163.1	172.57	27.68	2.68	9.47	2.68	5.806253832
1.9	50	188.3	198.9	52.88	2.88	10.6	5.76	5.629314923
2.3	75	214.33	225.53	78.91	3.91	11.2	5.213333333	5.225586712
2.9	100	236.88	236.88	101.46	1.46	0	1.46	0
1.1	0	136.35	145.1	0	0	8.75	0	6.417308398
1.5	25	163.92	172.79	27.57	2.57	8.87	10.28	5.411176184
1.9	50	191.35	199.01	55	5	7.66	10	4.003135615
2.3	75	215.05	224.19	78.7	3.7	9.14	4.933333333	4.250174378
2.9	100	237.16	237.16	100.81	0.81	0	0.81	0
1.1	0	136.42	145.19	0	0	8.77	0	6.428676147
1.5	25	163.5	172.71	27.08	2.08	9.21	8.32	5.633027523
1.9	50	190.3	199.17	53.88	3.88	8.87	7.76	4.661061482
2.3	75	215.45	223.96	79.03	4.03	8.51	5.373333333	3.94987236
2.9	100	237.16	237.16	100.74	0.74	0	0.74	0

The graphical presentation of experimental data shown in Fig. 20. Shows graphical representation of linearity and hysteresis.

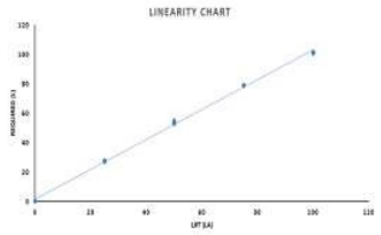

(a) Lift vs required length

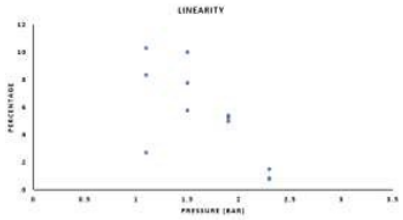

(b) Pressure vs required length

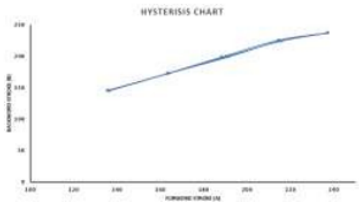

(c) Forward stroke vs backward stroke

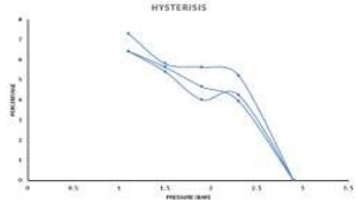

(d) Pressure vs percentage in hysteresis

Fig 20: Representation of linearity and hysteresis

Tianjin Daxue Xuebao (Ziran Kexue yu Gongcheng Jishu Ban)/
Journal of Tianjin University Science and Technology
ISSN (Online):0493-2137
E-Publication: Online Open Access
Vol: 55 Issue: 09:2022
DOI: 10.5281/zenodo.19248008

From Fig 20 (a-d) required length means the system is in the linear elastic region. This behaviour gives a straight line because the system resists deformation in a constant, predictable way. In the linear region, the material obeys Hooke's Law. The system behaves linearly with small or no hysteresis. When the forward stroke (A) and backward stroke increase over time due to required length and pressure, it typically means the system is experiencing mechanical or material changes under cyclic stress. When forward and backward stroke increase due to required length and pressure, but the percentage of hysteresis decreases, it means, The material or system is softening (losing stiffness).At the same time, internal friction or damping is reducing, so it loses less energy per cycle. As a result, stroke increases, but hysteresis loop area becomes smaller relative to total stroke. This often happens in fatigue testing as the material settles or degrades over time.

CONCLUSION

The material used in current study for analysis is SUP 9/SAE 5160 and 51CrV4. Shear stress and deformation calculated using FEA solver at position 85 of precompression, 50 mm stroke after precompression and 100 mm full stroke after precompression. Applied pressure on piston is 0.1320 MPa, 0.2097 MPa and 0.2874 MPa respectively. Shear stress and deformation at same positions shear stress calculated, as 447.35 N/mm^2, 730.68 N/mm^2, 1092.1 N/mm^2 for 50CrV4 and 395.63 N/mm^2, 628.27 N/mm^2, and 929.7 N/mm^2 for SUP 9/SAE 5160 and deformation are 87.95mm, 139.19mm, 189.94mm for 50CrV4. Deformations are 86.32mm, 136.53mm, 186.46mm for SUP 9/SAE 5160. Compared to SUP9/SAE 5160, 50CrV4 exhibits more shear stress and deformation due to its higher carbon content and its inclusion of chromium and vanadium, which enhance its strength and hardness. As a result, even under shear stresses, 50CrV4 can withstand greater loads before yielding or breaking. Shorter compression lengths the theoretical analysis closely approximates the FEA results as 85447.35 mm and 85449.1mm for spring with material 50CrV4 and 85395.63 mm and 85400 mm for spring with material SUP 9/SAE 5160.

Nomenclature

τ	-	Resultant shear stress
τ_F	-	Shear Stress due to Direct Force
τ_T	-	Shear Stress due to Torsion
F	-	Axial load on spring
D	-	Mean coil diameter
d	-	Wire diameter
K	-	Wahl correction factor
c	-	Spring index
k	-	Spring rate
y	-	Deformation
T_t	-	Throat length
$\Delta\boldsymbol{\varepsilon}$	-	Strain Range
e*, *p	-	Constants for Elastic and Plastic Region
n'	-	Elastoplastic Hardening Exponent
c'_f	-	fatigue ductility exponent

Tianjin Daxue Xuebao (Ziran Kexue yu Gongcheng Jishu Ban)/
Journal of Tianjin University Science and Technology
ISSN (Online):0493-2137
E-Publication: Online Open Access
Vol: 55 Issue: 09:2022
DOI: 10.5281/zenodo.19248008

σ'_f - Fatigue Ductility coefficient
b'_f - Fatigue Strength Exponent

References

1) Champagne, R.P. and Boyle, S.J., 1996. Optimizing valve actuator parameters to enhance control valve performance. ISA transactions, 35(3), pp.217-223.

2) Yang, C.J., Zhang, W.H., Ren, G.X. and Liu, X.Y., 2014. Modeling and dynamics analysis of helical spring under compression using a curved beam element with consideration on contact between its coils. Meccanica, 49, pp.907-917.

3) Della Pietra, L., 1976. The dynamic coupling of torsional and flexural strains in cylindrical helical springs. Meccanica, 11, pp.102-119.

4) Pietra, L.D. and Valle, S.D., 1982. On the dynamic behaviour of axially excited helical springs. Meccanica, 17(1), pp.31-43.

5) Wahl, A.M., 1963. Mechanical Springs. McGraw-Hill, New York.

6) Igor L Krivts, German V Krejnin, “Pneumatic Actuating Systems for Automatic Equipment Structure and Design”, Taylor & Francis Group, 2006

7) Wahl, A. M. "Analysis of effect of wire curvature on allowable stresses in helical Springs." (1939): A25-A30.

8) Cook, R.D., Young, W.C., 1985. Advanced Mechanics of Materials. Macmillan, New York.

9) Gzal, M., Groper, M. and Gendelman, O., 2017. Analytical, experimental and finite element analysis of elliptical cross-section helical spring with small helix angle under static load. International Journal of Mechanical Sciences, 130, pp.476-486.

10) Nagaya, K., 1987. Stresses in a helical spring of arbitrary cross section with consideration of end effects.

11) Keller, S.G. and Gordon, A.P., 2011. Equivalent stress and strain distribution in helical compression springs subjected to bending. The Journal of Strain Analysis for Engineering Design, 46(6), pp.405-415.

12) Jiang, W.G. and Henshall, J.L., 2000. A novel finite element model for helical springs. Finite elements in analysis and design, 35(4), pp.363-377.

13) Vogt, R.F., 1936. Stress and Deflection of Helical Springs. Transactions of the American Society of Mechanical Engineers, 58(6), pp.467-475.

14) Shigley, J.E., 2006. Mechanical Engineering Design, Eight Edition.

15) Zhang, D., Wang, G., Huang, F. and Zhang, K., 2020. Load-transferring mechanism and calculation theory along engaged threads of high-strength bolts under axial tension. Journal of Constructional Steel Research, 172, p.106153.

16) Fukuoka, T. and Nomura, M., 2008. Proposition of helical thread modeling with accurate geometry and finite element analysis.

17) Iso, B. and Standard, B.R.I.T.I.S.H., 2009. Mechanical properties of fasteners made of carbon steel and alloy steel. Bolts, screws and determined

18) Baran, R., Michalczyk, K. and Warzecha, M., 2023. Experimental analysis of transverse stiffness distribution of helical compression springs. acta mechanica et automatica, 17(1), pp.95-103.

19) Zebdi, O., Boukhili, R. and Trochu, F., 2009. Optimum design of a composite helical spring by multi-criteria optimization. Journal of reinforced plastics and composites, 28(14), pp.1713-1732.

Tianjin Daxue Xuebao (Ziran Kexue yu Gongcheng Jishu Ban)/
Journal of Tianjin University Science and Technology
ISSN (Online):0493-2137
E-Publication: Online Open Access
Vol: 55 Issue: 09:2022
DOI: 10.5281/zenodo.19248008

20) Gobbi, M. and Mastinu, G., 2001. On the optimal design of composite material tubular helical springs. Meccanica, 36, pp.525-553.

21) Del Llano-Vizcaya, L., Rubio-Gonza´lez, C.,Mesmacque, G., and Cervantes- Herna´ndez, T. Multiaxial fatigue and failure analysis of helical compression springs. Engng Failure Analysis, 2006,13, 1303–1313.

22) Akiniwa Y., Stanzl-Tschegg S., Mayer H., Wakita M., and Tanaka K., “fatigue strength of spring steel under axial and torsional loading in the very high cycle regime”, international journal of fatigue, elsevier, vol. 30, pp. 2057-2063

23) Berger, C. and Kaiser, B., 2006. Results of very high cycle fatigue tests on helical compression springs. International journal of fatigue, 28(11), pp.1658-1663.

24) Todinov, M.T., 1999. Maximum principal tensile stress and fatigue crack origin for compression springs. International Journal of Mechanical Sciences, 41(3), pp.357-370.

25) Melander, A. and Larsson, M., 1993. The effect of stress amplitude on the cause of fatigue crack initiation in a spring steel. International Journal of Fatigue, 15(2), pp.119- 131.

26) Gomes, V.M., Souto, C.D., Correia, J.A. and de Jesus, A.M., 2024. Monotonic and Fatigue Behaviour of the 51CrV4 Steel with Application in Leaf Springs of Railway Rolling Stock. Metals, 14(3), p.266.

27) Bannantine, J.A., Comer, J.J. and Handrock, J.L., 1990. Fundamentals of metal fatigue analysis.

28) Ellyin, F., 2012. Fatigue damage, crack growth and life prediction. Springer Science & Business Media.

29) Jhansale, H.R. and Topper, T.H., 1971. Engineering analysis of the inelastic stress response of a structural metal under variable cyclic strains. In Cyclic stress-strain behavior—Analysis, experimentation, and failure prediction. ASTM International.

30) Li, D.M., Nam, W.J. and Lee, C.S., 1998. A strain energy-based approach to the low- cycle fatigue damage mechanism in a high-strength spring steel. Metallurgical and Materials Transactions A, 29, pp.1431-1439.

31) Dutta, A., Dhar, S. and Acharyya, S.K., 2010. Material characterization of SS 316 in low-cycle fatigue loading. Journal of Materials Science, 45, pp.1782-1789.

32) Srinivasan, V.S., Sandhya, R., Rao, K.B.S., Mannan, S.L. and Raghavan, K.S., 1991. Effects of temperature on the low cycle fatigue behaviour of nitrogen alloyed type 316L stainless steel. International journal of fatigue, 13(6), pp.471-478.

33) Das, B. and Singh, A., 2019. Understanding strain controlled low cycle fatigue response of P91 steel through experiment and cyclic plasticity modeling. Fusion Engineering and Design, 138, pp.125-137.

34) Shankar, V., Bauer, V., Sandhya, R., Mathew, M.D. and Christ, H.J., 2012. Low cycle fatigue and thermo-mechanical fatigue behavior of modified 9Cr–1Mo ferritic steel at elevated temperatures. Journal of nuclear materials, 420(1-3), pp.23-30.

35) Niesłony, A., el Dsoki, C., Kaufmann, H. and Krug, P., 2008. New method for evaluation of the Manson–Coffin–Basquin and Ramberg–Osgood equations with respect to compatibility. International Journal of Fatigue, 30(10-11), pp.1967-1977.

36) Ramberg, W. and Osgood, W.R., 1943. Description of stress-strain curves by three parameters (No. NACA-TN-902).

37) Indi-Tech Valve Design Data (Datasheet for actuator design, R&D), 2023-24

38) ASME B16.34-2020, American Society of Mechanical Engineers.

39) ASME SEC VIII DIV 1-2021, American Society of Mechanical Engineers